Lyotropic Phase Behavior and Structure of Mixed Lipid (POPC)−Detergent ($C_{12}E_n$, $n = 2$, 4, 6) Assemblies: Insights from Hydration-Tuning Infrared Spectroscopy

Hans Binder* and Gotthard Klose†

University of Leipzig, Interdisciplinary Centre for Bioinformatics, Kreuzstrasse 7b, D-4103 Leipzig, Germany

Received: June 27, 2002; In Final Form: August 13, 2002

The work is aimed to understand the effect of nonionic surfactants on the stability of lipid membranes and to characterize the aggregate structure on a molecular level. We studied the lyotropic phase behavior of mixtures of the lipid 1-palmitoyl-2-oleoyl-sn-glycero-3-phosphocholine (POPC) with nonionic surfactants of the homologous series $C_{12}E_n$ ($n = 2$, 4, 6) as a function of composition (up to a mole ratio detergent-to-lipid, $R_{D/L} = 1$), temperature (0 °C < T < 50 °C), and relative humidity (3% < RH < 100%). The latter parameter was used to adjust and to vary the hydration degree of the samples. The results were summarized in terms of RH−T phase diagrams. At full hydration (RH = 100%), all systems formed mixed bilayers. The studied nonionic detergents promoted the formation of the inverse hexagonal phase, H_{II}, at reduced hydration and above a critical temperature near 20 °C, i.e., in the left upper corner of the phase diagram. Solid phases were observed at lower temperatures. $C_{12}E_2$ showed some special properties. This detergent with a short ethylene oxide (EO) chain stabilized the solid phase at low concentrations, and it extended the range of the H_{II} phase to higher RH as compared with the effect of the detergents with longer EO chains. The different phases were characterized in terms of molecular order and conformational properties of the EO chains. In membranes, they existed in a more ordered state than in assemblies of the pure detergent at equal external conditions. In a methodical respect, this work demonstrates that hydration-tuning infrared linear dichroism spectroscopy is well-suited to detect phase transitions of lipid/detergent mixtures between fluid and solid structures and between aggregates of lamellar and nonlamellar morphologies.

Introduction

Lipids and nonionic surfactants of the ethylene oxide (EO) type belong to amphiphiles, which, in general, exhibit a rich phase behavior depending on the nature of the molecules, on their hydration degree, and on the external conditions given by means of temperature and pressure. Phase transitions reveal microscopic characteristics of amphiphilic systems on a macroscopic level. For example, transitions between lamellar and nonlamellar phases manifest the imbalance of lateral forces acting between the constituents at different depths within the bilayer. Consequently, investigations on the phase behavior of assemblies of amphiphilic molecules open up the opportunity to study factors that affect their stability in a systematic fashion.

The temperature can be easily adjusted and controlled within an experimental setup. Thermotropic (temperature-dependent) studies are therefore frequently realized. Temperature, however, suffers from the disadvantage that changes of this variable result in simultaneous alterations in volume, intermolecular interactions, and thermal energy, which makes it difficult to disentangle these contributions. Alternatively, one can vary the external (hydrostatic) pressure at constant temperature.[1−4] Such barotropic experiments permit the isolation of effects that depend on changes in volume. Consequently, this method provides a direct approach to molecular interactions, which depend directly on intermolecular distances and molecular conformations.

As a third option, one can modulate the properties of amphiphilic systems by alteration of their hydration degree. Such lyotropic experiments provide a direct access to study the role of water for the stability and structure of molecular aggregates. Note that hydration studies provide information not only on water binding characteristics but also on elastic properties of amphiphilic aggregates[5−7] and their phase behavior.[8,9]

The present study deals with the effect of detergents of the homologous series $C_{12}E_n$ ($n = 2$, 4, 6) on membranes of the monounsaturated lipid 1-palmitoyl-2-oleoyl-sn-glycero-3-phosphocholine (POPC). We investigated the phase behavior of lipid/detergent mixtures as a function of concentration, temperature, and relative humidity (RH) using infrared (IR) linear dichroism spectroscopy in combination with the so-called humidity titration technique, which was used to adjust the hydration degree of the samples with high precision and reproducibility. One special advantage of humidity-tuned IR linear dichroism spectroscopy should be recognized in its capacity to detect phase transitions with high sensitivity.

The results were summarized in terms of RH−T phase diagrams. The different phases were characterized in terms of molecular order and conformation of the methylene and EO chains. A following paper will focus on the interpretation of the phase behavior in terms of monolayer bending and local hydration properties of the polar interface of the mixed lipid/detergent assemblies.

Materials and Methods

Materials. The lipid POPC was purchased from Avanti Polar Lipids, Inc. (Alabaster, AL). The oligo(EO) dodecyl ethers of

* To whom correspondence should be addressed.Tel: +49 341-149510. Fax: +49-341-1495-119. E-mail: binder@rz.uni-leipzig.de.

† Universität of Leipzig, Institute of Experimental Physics I, Linnèstrasse 5, D-4103 Leipzig, Germany.

10.1021/jp0263929 CCC: $22.00
Published on Web 09/26/2002

the general type $C_{12}H_{25}(CH_2CH_2O)_nH$ ($C_{12}E_n$; $n = 2, 4, 6$) were provided by Nikko Chemicals (Tokyo, Japan). The compounds were of high purity and were used without further treatment. The deuteration of the EO chains in $C_{12}H_{25}(CD_2CD_2O)_nH$ ($C_{12}E_n$-d_{4n}) was realized by etherification[10] of the respective perdeuterated *n*-(oxyethylene) glycol (synthesized as described in ref 11) and $CH_3(CH_2)_{11}Br$. The perdeuterated alkyl chain analogue $C_{12}D_{25}(CH_2CH_2O)_4H$ ($C_{12}E_4$-d_{25}) and the partially deuterated analogues $C_{11}H_{23}CD_2(CH_2CH_2O)_nH$ ($C_{12}E_n$-d_2) were synthesized by etherification of tetraethylene glycol and $CD_3(CD_2)_{11}Br$ and $CH_3(CH_2)_{10}CD_2Br$, respectively (euriso-top, France). Sample solutions were prepared by dissolving the components at definite molar ratios detergent-to-lipid, $R_{D/L}$, in methanol.

IR Measurements. Appropriate amounts of the stock solution were spread on the surface of a ZnSe-attenuated total reflection (ATR) crystal for sample preparation (angle of incidence, 45°; six active reflections). The solvent evaporates under a stream of nitrogen within a time of less than some minutes. The amount of material corresponds to an average thickness of the lipid films of >3 μm, or equivalently, to a stack of >500 bilayers in the lamellar phase. Polarized IR absorption spectra, $A_{||}(\nu)$ and $A_{\perp}(\nu)$, were recorded with light polarized parallel and perpendicular with respect to the plane of incidence (128 accumulations each) using a BioRad FTS-60a Fourier transform IR spectrometer (Digilab, MA) equipped with a wire grid polarizer. Band positions were analyzed by means of their center of gravity (COG) in the weighted sum spectrum, $A(\nu) = A_{||}(\nu) + 2.55A_{\perp}(\nu)$.

The IR order parameter of an absorption band was calculated from the dichroic ratio of the integral, baseline-corrected polarized absorbances, $R = A_{||}/A_{\perp}$ using Harricks thick film approximation[12] (see also ref 13 for details):

$$S_{IR} = (R - 2)/(R + 2.55) \quad (1)$$

It is defined as the mean second order Legendre polynomial, $S_{IR} \equiv < 0.5(3\cdot\cos^2\theta_{\mu n} - 1)>$, where $\theta_{\mu n}$ is the angle between the respective transition moment, μ, and the ATR normal, n. The molecular ordering of the hydrocarbon chains can be estimated using the IR order parameters of the symmetric and antisymmetric CH_2 stretching bands, $S_{IR}(\nu_s(CH_2))$ and $S_{IR}(\nu_{as}(CH_2))$, respectively. Their transition moments are assumed to point perpendicular to one another and perpendicular to the fiber axis of the methylene chain. Consequently, both parameters can be combined to yield the apparent longitudinal order parameter of the chains according to[13,14]

$$S_\theta = -(S_{IR}(\nu_s(CH_2)) + S_{IR}(\nu_{as}(CH_2))) \quad (2)$$

It provides a measure of the mean segmental order parameter of the methylene chain according to $S_\theta \propto <0.5(3\cdot\cos^2\theta_{zn} - 1)>$, where θ_{zn} denotes the angle enclosed between the ATR normal, n, and the interconnecting line between the midpoints of two successive C−C bonds (segmental axes, see ref 14 for details).

The IR chain order parameter can be written in the form

$$S_\theta = S_d \cdot S_m \quad (3)$$

for uniaxially symmetric molecular assemblies. S_d and S_m are defined as the second-order Legendre polynomials of the angle enclosed between the local director and the ATR normal (S_d) and between the local director and the segmental axes (S_m). Here, S_d represents a measure of the degree of macroscopic ordering with respect to the ATR surface, whereas S_m quantifies the segmental ordering relative to the director of the molecular aggregate. The order parameter of macroscopic orientation scales the segmental order parameter S_m. For different simple aggregate morphologies, one obtains $S_d = 1$ (membranes aligned parallel to the ATR surface), $S_d = 0.25$ (cylinders with their axes parallel to the ATR surface), and $S_d = 0$ (spheres).[9] Hence, the bending of lipid lamellae into aggregates with a curved surface morphology is expected to cause a significant drop of the absolute value of S_θ because its nonlamellar shape does not match with the plane ATR surface.

Humidity Titration Technique. The hydration degree of the lipid film was adjusted by means of the humidity titration technique, which has proved to be practical, relatively fast to achieve, accurate, and, last but not least, well-defined in a thermodynamic sense.[15,8] The method is called humidity titration because water vapor is "injected" in definite portions of the RH into the sample chamber.

In particular, high purity nitrogen gas of a definite RH was blown through the sample chamber. The temperature (T) and RH were adjusted by means of a flowing water thermostat (Julabo, Seelbach, Germany) and a moisture generator (Humi-Var, Leipzig, Germany) with an accuracy of ± 0.05 K and $\pm 0.5\%$ RH, respectively. The RH was increased in steps of ΔRH $= 3\%$ from 5 to 98% (hydration scan) or decreased in the opposite direction (dehydration scan) at constant T. In some cases, heating/cooling scans were performed by increasing/decreasing T in steps of $\Delta T = 1$ K at RH = constant.

The sample was allowed to equilibrate for 10 min in RH scans and for 2 min in temperature scans before measurement of the polarized IR spectra. No significant hysteresis effects between hydration and dehydration scans and between heating and cooling scans were detected confirming that the sample reached equilibrium in each measurement.

Results and Discussion

IR Spectra of POPC/$C_{12}E_n$ Mixtures. Figure 1 shows IR spectra of the investigated samples, of detergents of the $C_{12}E_n$ type, of the phospholipid POPC, and of the equimolar mixture POPC/$C_{12}E_4$. Characteristic absorption bands can be assigned to IR active vibrations of atomic groups of both components, which reside in different regions of the molecular assemblies and of the adsorbed water. For example, the O−H stretches of water and of the terminal hydroxyl groups of the EO chains give rise to a broad feature in the 3700−3100 cm^{-1} range. The C═O stretching vibration of the carbonyl groups and the antisymmetric stretches of the phosphodiester groups of the lipid protrude near 1730 cm^{-1} (ν(C═O)) and 1230 cm^{-1} ($\nu_{as}(PO_2^-)$), respectively. These modes characterize the polar region of the studied systems.

Several absorption bands originate from vibrations of the methylene groups, which are predominantly located within the aliphatic chains of the lipid and the detergent and thus within the hydrophobic region of the aggregates (see also Figure 2). To characterize the detergent alkyl chains by means of the methylene vibrations, one has to consider that also the CH_2 units in the EO chains contribute to the respective absorption bands. Figure 2 shows the C−H and C−D stretching regions of $C_{12}E_4$-d_{16} and of $C_{12}E_4$-d_{25} with selectively deuterated EO and alkyl chains, respectively. Note that deuteration shifts the methylene stretches downward by more than 700 cm^{-1}. This way, the CH_2 modes of the EO methylenes are filtered out in the spectrum of $C_{12}E_4$-d_{25} whereas the CH_2 modes of the alkyl methylenes are separated in the spectrum of $C_{12}E_4$-d_{16}. Com-

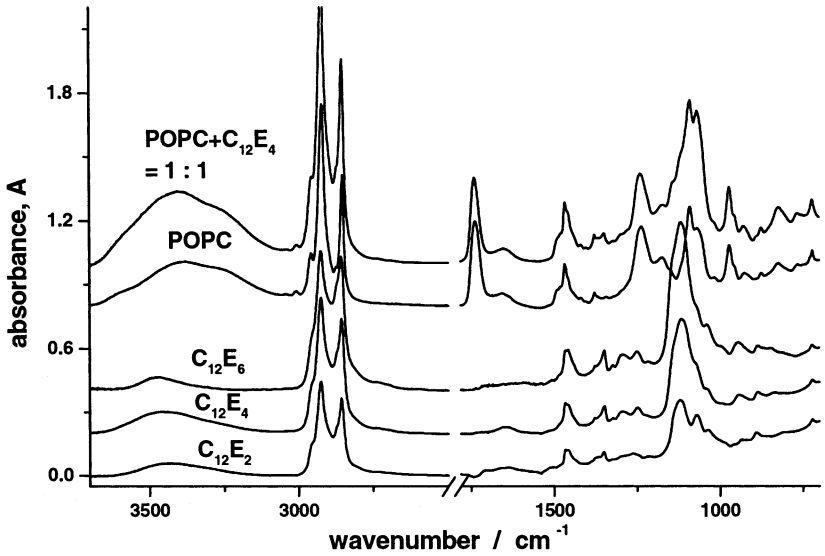

Figure 1. IR sum spectrum, $A = A_{||} + 2.55A_{\perp}$, of the detergents, $C_{12}E_n$ ($n = 2, 4, 6$), of the lipid POPC and of the equimolar mixture POPC/$C_{12}E_4$ ($T = 25$ °C, RH = 50%).

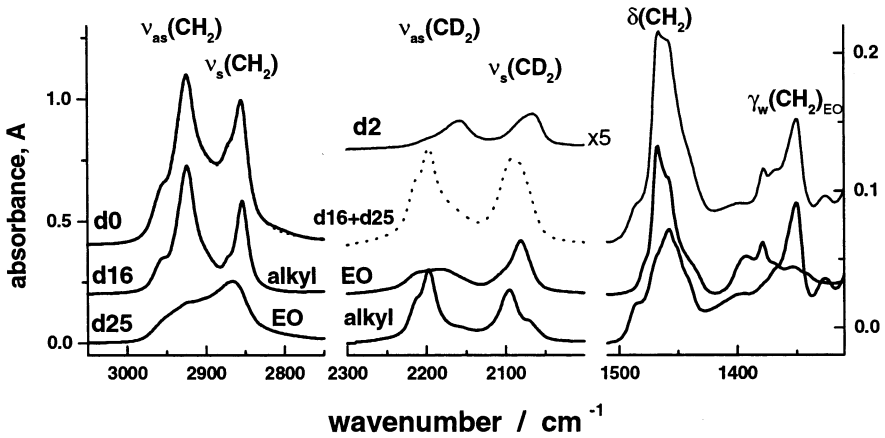

Figure 2. Selected regions of the IR sum spectrum, which are mainly due to vibrations of the methylene groups: $C_{12}E_4$-d_{25} (d_{25}: proteated EO chain and deuterated alkyl chain), $C_{12}E_4$-d_{16} (d_{16}: proteated alkyl chain and deuterated EO chain), $C_{12}E_4$-d_0 (d_0: proteated EO and alkyl chains), and $C_{12}E_4$-d_2 (d_2: deuterated α-methylene group). For assignments, see text. The dotted spectrum, "$d_{16} + d_{25}$", represents the calculated sum of "d_{16}" and "d_{25}". The calculated sum "$d_{16} + d_{25}$" and the measured "d_0" spectrum are not discernible in the region of the CH_2 stretching bands. This result indicates the absence of significant isotope effects on structural properties.

parison of both spectra shows that the symmetrical CH_2 stretching vibration of the EO methylenes, $\nu_s(CH_2)_{EO}$, absorbs at higher wavenumbers than the respective mode of the alkyl methylenes, $\nu_s(CH_2)$. Moreover, the antisymmetric mode, $\nu_{as}(CH_2)_{EO}$, is distinctly broader than $\nu_{as}(CH_2)$. Consequently, the peaks near 2850 and 2920 cm^{-1} in the spectrum of the completely proteated surfactant can be mainly assigned to methylene stretches of the alkyl methylenes. They are only weakly distorted by the EO methylenes except for a systematic shift of the COG, COG($\nu_s(CH_2)$), of about 1 cm^{-1} and a distinct broadening (cf. Figure 2, spectrum "d_0"). To minimize interference of the EO units with the absorbance of the aliphatic methylenes, we calculated the integral polarized absorbances within the spectral range with absorbances greater than 75% of the maximum height. The maximum positions of the CD_2 stretching bands of $C_{12}E_4$-d_2 (with deuterated α-methylenes) clearly deviated from that of $C_{12}E_4$-d_{25}. We concluded that our analysis in terms of IR order parameters characterized segmental ordering of the alkyl chains except that of the α-methylenes.

The absorption band at about 1351 cm^{-1}, evident in the spectrum of completely proteated $C_{12}E_4$-d_0 and of $C_{12}E_4$-d_{25}, was assigned to the deformation mode of the EO methylenes mainly due to their wagging vibration, $\gamma_W(CH_2)_{EO}$[16] (cf. Figure 2). As expected, this band disappeared for $C_{12}E_4$-d_{16}. There was virtually no overlap with absorption bands of POPC of comparable intensity. Consequently, the $\gamma_W(CH_2)_{EO}$ band was suited to characterize the ordering of the EO chains (vide infra).

Lyotropic Phase Transitions of Lipid/Detergent Mixtures. The mean wavenumber of the stretching bands of aliphatic methylenes and their linear dichroism sensitively depend on the mean conformational state of the hydrocarbon chains and on the morphology of the molecular aggregates.[15] Typically, disordered, fluid chains are characterized by values of the COG of the symmetric CH_2 stretching band of COG($\nu_s(CH_2)$) > 2852 cm^{-1} whereas frozen chains in the all trans conformation show smaller wavenumbers of COG($\nu_s(CH_2)$) < 2852 cm^{-1}. For lipid bilayers, the alteration of band position is accompanied by a change of the IR chain order parameter, S_θ, which drops from $S_\theta > 0.5$ to $0.3 < S_\theta < 0.5$ if the lamellae undergo the transition from the solid into the liquid crystalline phase. On the other hand, nonlamellar fluid and lamellar fluid phases are both characterized by disordered methylene chains with relatively high COG($\nu_s(CH_2)$) values. The different aggregate morphologies, however, cause differences of the respective IR order

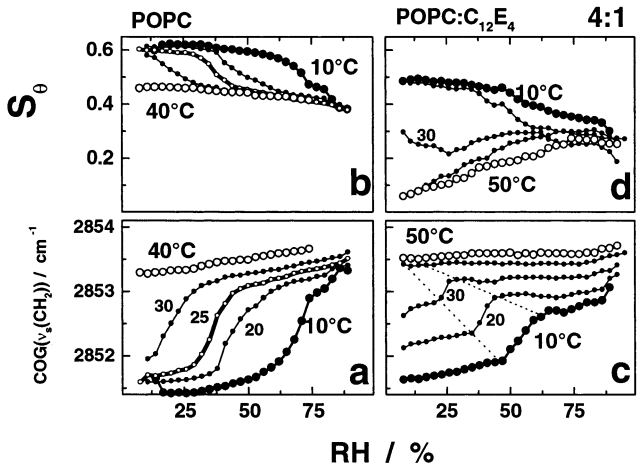

Figure 3. Segmental IR order parameter of the aliphatic chains, S_θ, and the COG of the $\nu_s(CH_2)$ band, COG($\nu_s(CH_2)$), of POPC (parts a and b) and of the mixture POPC/$C_{12}E_4$ ($R_{D/L} = 0.25$) at different temperatures as a function of the RH. The dotted lines indicate the onset and completion of chain melting.

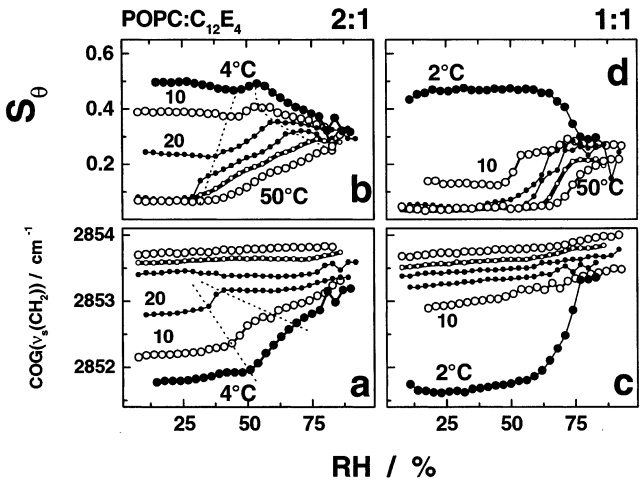

Figure 4. Segmental IR order parameter of the aliphatic chains, S_θ, and the COG of the $\nu_s(CH_2)$ band, COG($\nu_s(CH_2)$), of the mixtures POPC/$C_{12}E_4$ ($R_{D/L} = 0.5$ and 1) at different temperatures as a function of the RH.

parameters. Nonlamellar phases of curved, monolayer-related structures such as the inverse hexagonal (H_{II}), the micellar, and the cubic phases are correlated with smaller values of S_θ than liquid crystalline lamellae (see eq 3). Consequently, the combination of these two observations of the IR linear dichroism experiment, the COG of the symmetric CH_2 stretching band, and the chain order parameter unambiguously enables the identification of transitions between solid and fluid phases on one hand and of transitions between lamellar and nonlamellar phases on the other hand in a relatively simple fashion and with high precision.[9,17]

For example, the sigmoidal alterations of the COG of the symmetric CH_2 stretching band, COG($\nu_s(CH_2)$), and of the respective chain order parameter, S_θ, as a function of RH indicate the lyotropic gel to liquid crystalline lamellar phase transition of the pure lipid POPC in the intermediate RH range. Its mean position shifts to smaller RH upon heating (see Figure 3a,b).

The mixed $C_{12}E_4$/POPC systems show a similar behavior as the pure lipid at low temperatures (see Figures 3c,d and 4). At higher temperatures, the chain order parameter progressively decreases with dehydration. The respective mean wavenumber,

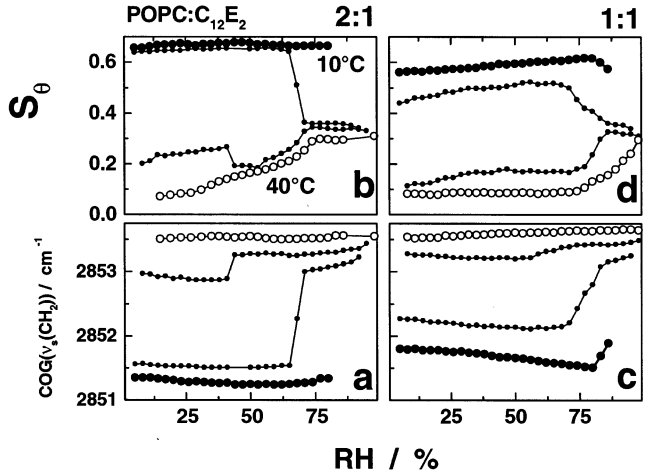

Figure 5. Segmental IR order parameter of the aliphatic chains, S_θ, and the COG of the $\nu_s(CH_2)$ band, COG($\nu_s(CH_2)$), of the mixtures POPC/$C_{12}E_2$ ($R_{D/L} = 0.5$ and 1) at different temperatures as a function of RH.

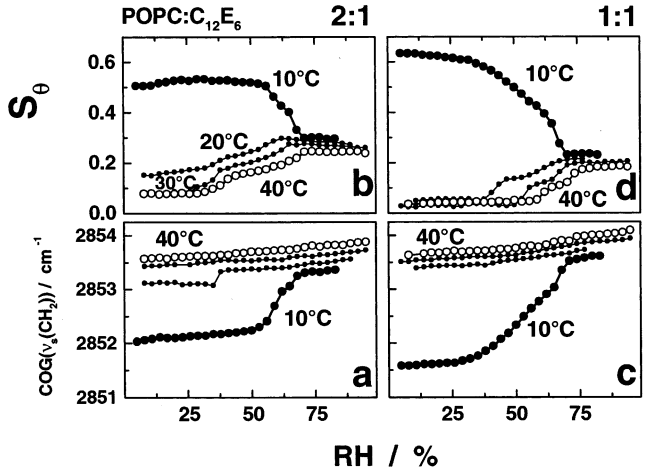

Figure 6. Segmental IR order parameter of the aliphatic chains, S_θ, and the COG of the $\nu_s(CH_2)$ band, COG($\nu_s(CH_2)$), of the mixtures POPC/$C_{12}E_6$ ($R_{D/L} = 0.5$ and 1) at different temperatures as a function of RH.

COG($\nu_s(CH_2)$), indicates the existence of molten chains at these conditions. These results can be interpreted in terms of a transition from lamellar fluid into nonlamellar structures, which form upon dehydration in the range of low RH. The ternary phase diagram of POPC/$C_{12}E_4$/water ($T = 25$ °C) predicts the inverse hexagonal phase (H_{II}) for $R_{D/L} = 1$ and phase coexistence between the gel and the H_{II} phases between about $R_{D/L} = 0.5$ and 0.25 at low water content in agreement with our interpretation of the IR results.[18] In these systems, the observed intermediate values of COG($\nu_s(CH_2)$) and S_θ indeed reflect H_{II}/gel phase coexistence. They can be rationalized in terms of weighted averages of the respective spectral parameter originating from nonlamellar fluid and lamellar solid domains (vide infra). A direct transition between the lamellar gel and the inverse hexagonal phase has been described previously for pure, partly hydrated lipids.[19,9]

We observed similar phase transitions if $C_{12}E_4$ is substituted by $C_{12}E_2$ (Figure 5) and $C_{12}E_6$ (Figure 6). Funari et al.[20] found gel−H_{II} phase coexistence in POPC/$C_{12}E_2$ mixtures ($R_{D/L} = 0.5$ and 1) at $T = 25$ °C in the same RH range in which our IR data indicate the coexistence between the gel and a nonlamellar phase (see also ref 21). X-ray diffraction studies on POPC/$C_{12}E_n$ mixtures ($n = 2, 4, 6$; $R_{D/L} = 1, 0.5$) at different temperatures and relative humidities confirm the assignment of phases and in particular the existence of the inverse hexagonal phase in all

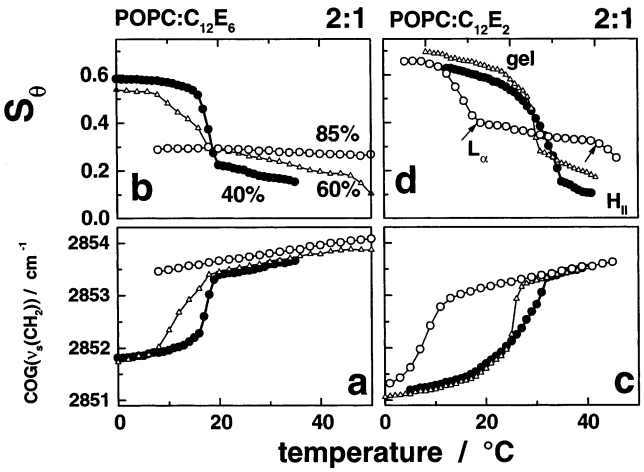

Figure 7. Segmental IR order parameter of the aliphatic chains, S_θ, and the COG of the $\nu_s(CH_2)$ band, COG($\nu_s(CH_2)$), of the mixtures POPC/$C_{12}E_n$ ($n = 2$, 6; $R_{D/L} = 0.5$) at different RHs (see part b) as a function of temperature.

investigated mixtures at small RH values (Islamov, A.; Klose, G. Personal communication).

The chain order parameter, S_θ, shown in Figures 3−6 represents a spectroscopic mean over the methylene groups of the palmitoyl and oleoyl chains of POPC and of the dodecyl chains of the detergent; thus, it characterizes the mean segmental order within the hydrophobic region of the amphiphilic aggregates (see also ref 14). Extrapolation to RH = 100% provides values of $S_\theta \approx 0.4$ in liquid crystalline membranes of pure POPC and of slightly smaller values of about $S_\theta \approx 0.3$ in mixed membranes. Hence, addition of the detergent decreases the mean segmental order within the hydrophobic core. The values of the IR chain order parameter, S_θ, can be compared with the mean segmental ^{2}H NMR order parameter, $S_{NMR} = -2\langle S_{CD}\rangle_{chain}$. Here, S_{CD} is the C−D bond order parameter and the angular brackets denote averaging over all deuterated methylene groups of the considered chains.[22] The relevant value of S_{NMR} was estimated from the respective order parameter profiles of the palmitoyl and oleoyl chains of POPC and of the dodecyl chains of the detergent, which were taken from refs 9 and 23. The obtained mean NMR order parameter is systematically smaller by about 10−30% as compared with the respective IR order parameter, but it decreases in a similar fashion as S_θ upon addition of detergent. The systematical difference between IR and NMR chain order parameters can be explained by reorientations of methylene segments within the characteristic time scale of the NMR experiment ($>10^{-6}$ s). Note that the considered IR order parameter is virtually not affected by dynamic effects owing to the relatively small time scale of IR absorption ($<10^{-11}$ s).

Temperature Scans and the Stability of the Solid Phase. Heating scans of the pure components and of selected mixtures were performed at constant RH (selected scans of the binary systems were shown in Figure 7). The temperature behavior of the spectral parameters COG($\nu_s(CH_2)$) and S_θ provides a consistent picture together with the results of the dehydration scans presented above. At RH = 40%, the mixtures melt from the gel state directly into the H_{II} phase as indicated by the marked alteration of band position and order parameter. The temperature scan of POPC/$C_{12}E_2$ shows the phase sequence gel → L_α → H_{II} at RH = 85%. Here, the liquid crystalline lamellar L_α phase is characterized by "intermediate" values of the chain order parameter (see arrows in Figure 7d).

The maximum of the first derivative of the COG of the CH_2 stretches provides an appropriate measure of the characteristic temperature of the hydrocarbon chain melting transition (Figure 8). The melting transition of pure $C_{12}E_6$ takes place at a higher temperature than the transition of the detergents with shorter

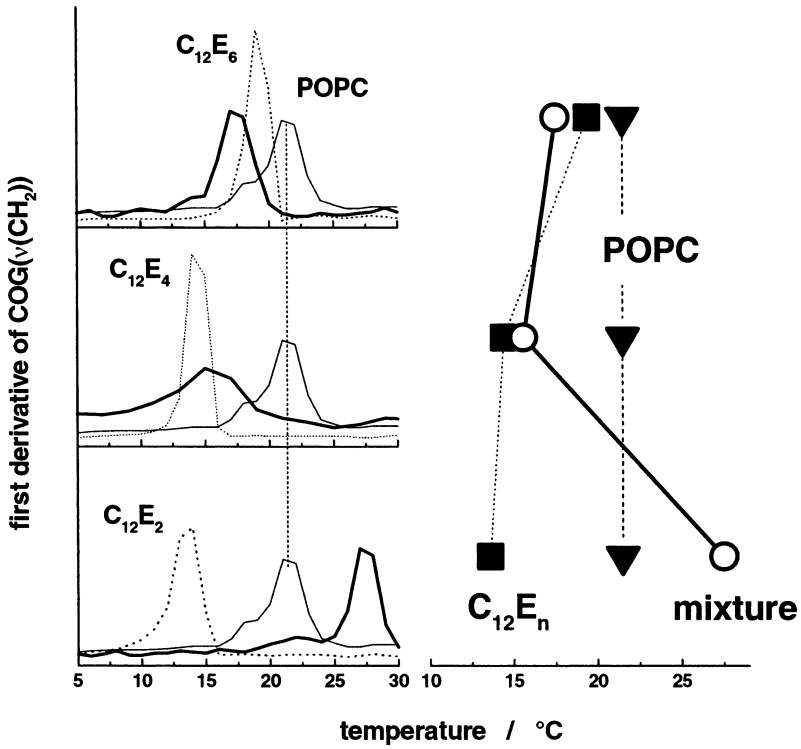

Figure 8. Left: Solid−fluid phase transitions of pure POPC (thin solid graphs), of pure detergents $C_{12}E_m$ ($m = 2$, 4, 6; dotted lines), and of 2:1 mixtures POPC/$C_{12}E_m$ ($R_{D/L} = 0.5$, thick solid curves) at RH = 50%. The graphs show the first derivative of the COG with respect to temperature, ∂COG($\nu(CH_2)$)/∂T, as a function of temperature. Right: Plot of the respective phase transition temperature (maximum positions of the peaks shown on the left) for the detergents and their mixture with POPC.

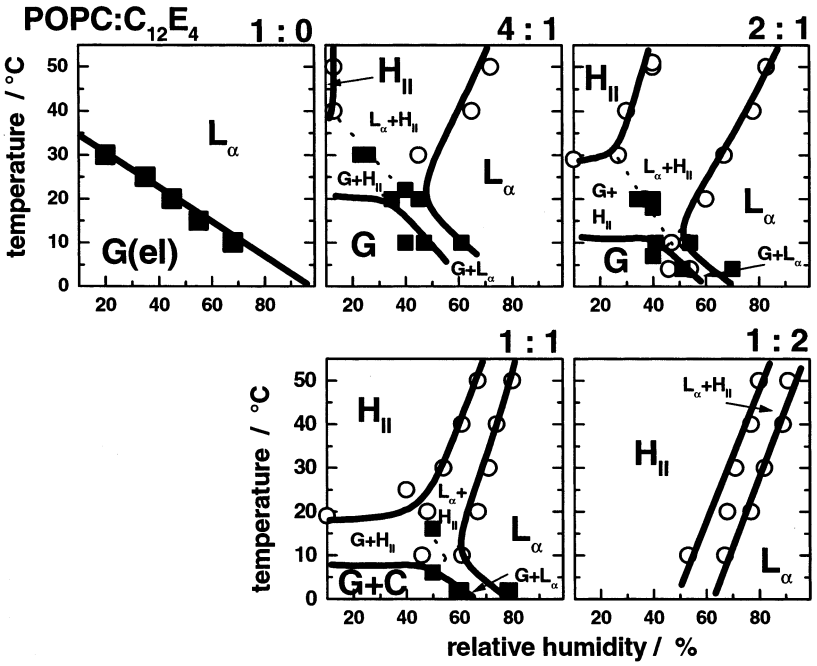

Figure 9. RH-T phase diagrams of POPC and of POPC/$C_{12}E_4$ mixtures ($R_{D/L}$ = 0.25, 0.5, 1, 2). Phase boundaries were determined from the onset and completion points of the sigmoidal changes of IR parameters (see Figures 3 and 4). Solid squares refer to chain melting transitions (gel/liquid crystalline) and open circles refer to nonlamellar−lamellar transitions. Three phase coexistence is shown by dotted lines. They are partly hypothetical because of experimental uncertainty. The gel, liquid crystalline, and inverse hexagonal phase are denoted by G, L_α, and H_{II}, respectively. Phase coexistence of the lipid-rich gel with crystalline detergent is denoted by G + C. See text.

EO chains. Longer EO chains stabilize the solid phase of pure detergents indicating an energetically favorable molecular conformation and/or packing mode. Figure 8 also compares the respective characteristics of the pure components with that of 2:1 mol/mol lipid/detergent mixtures. If the systems were heated at RH = 50%, the melting transition of the POPC/$C_{12}E_2$ system takes place at a higher temperature (27 °C) than the melting transition of the pure components, POPC (22 °C) and $C_{12}E_2$ (14.5 °C). The higher stability of the gel phase of the mixture indicates favorable cross-interactions between the lipid and the detergent. Contrarily, addition of $C_{12}E_6$ slightly decreases the transition temperature of the mixture as compared with the transition temperature of the pure components. The longer EO chains obviously give rise to unfavorable cross-interactions; thus, they destabilize the solid phase of the mixture.

RH-T Phase Diagrams of POPC and of POPC/$C_{12}E_n$ (*n* = 2, 4, 6) Mixtures. On the basis of the phase transition data, which were obtained from the RH and temperature scans and the respective spectral analyses, we are able to construct the RH-T phase diagrams of POPC and of POPC/$C_{12}E_n$ mixtures (Figures 9 and 10).We assigned the nonlamellar phase to H_{II} in accordance with X-ray and NMR experiments[18,24,20] (Islamov, A.; Klose, G. Personal communication).

Pure POPC progressively hydrates with increasing RH until the RH reaches a critical value at which the lipid transforms from the gel into the liquid crystalline lamellar phase. The transition is expected to proceed at one value of RH=RH^{tr} under isobaric−isothermal conditions according to the condition of equal chemical potential of water in the coexisting phases.[25] In reality, the transition spans a RH range of about 5−10%, which represents a sort of intrinsic width. The observed transition width remains virtually unchanged at slower scan rates, in scans of reversed direction (hydration), with different amounts of material and with lipid of different manufacturers (impurities). We considered the transition width of pure POPC as reference for comparison with the lipid/detergent mixtures and used its center

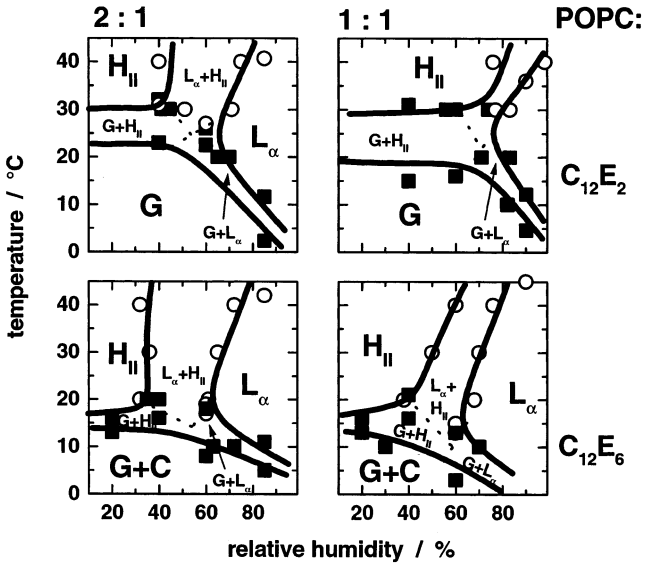

Figure 10. RH-T phase diagrams of POPC/$C_{12}E_2$ and POPC/$C_{12}E_6$ mixtures ($R_{D/L}$ = 0.5, 1). See Figure 9 caption for details.

as the respective transition value, RH^{tr}. It increased with decreasing temperature as indicated by the negative slope of the gel/L_α coexistence line in the phase diagram (Figure 9). We recently found indications of a nonlamellar phase of POPC at RH < 15% and T > 35 °C,[17] which are not considered here.

Addition of detergent increases the number of components in the mixture; thus, the binary lipid/detergent mixture possesses one additional thermodynamic degree of freedom. Now, the system is expected to pass a two phase region upon phase transformation. The respective transition ranges are indeed considerably broader than that of the pure lipid. In the transition range, the composition detergent-to-lipid, $R_{D/L}$, and the hydration degree water-to-lipid, $R_{W/L}$, of both coexisting phases alter as a function of RH. The respective adsorption isotherms of POPC

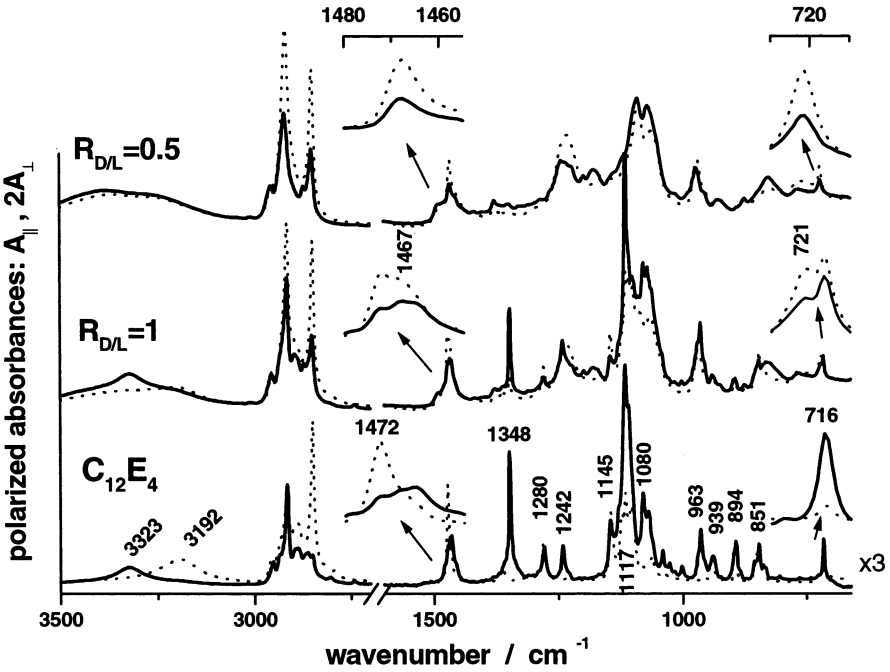

Figure 11. Polarized IR spectra, $A_{||}(\nu)$ and $2A_{\perp}(\nu)$, of the detergent $C_{12}E_4$ and of POPC/$C_{12}E_4$ mixtures with $R_{D/L} = 0.5$ and 1 ($T = 4$ °C, RH = 50%). The insertions amplify the spectral regions of the $\delta(CH_2)$ and $\gamma_R(CH_2)$ bands (see text). Note that equal intensities of both spectra, $A_{||} = 2A_{\perp}$, correspond to $S_{IR} = 0$ whereas $A_{||} > 2A_{\perp}$ and $A_{||} < 2A_{\perp}$ refer to $S_{IR} > 0$ and $S_{IR} < 0$, respectively (see eq 1). The numbers indicate the peak positions of selected bands in units of cm^{-1} (see Table 1 for assignments).

and of POPC + $C_{12}E_n$ (not shown) indicate that the chain melting transition is paralleled by the adsorption of 0.5−1 water per lipid. A detailed analysis of the water binding capacity in terms of $R_{W/L}$ and phase structure will be published elsewhere (Binder, H. Manuscript in preparation).

After the RH is increased, the lipid/detergent mixtures can pass two two phase coexistence ranges, which are separated by a critical RH value of three phase coexistence according to the sequence gel → gel + H_{II} → gel + H_{II} + L_α → H_{II} + L_α → L_α at T = constant. In the RH-T phase diagram, two phase coexistence consequently refers to an area whereas three phase coexistence is predicted along a line according to the Gibbs phase rule. Note that both used IR parameters, COG($\nu_s(CH_2)$) and S_θ, are sensitive to gel + H_{II} coexistence whereas only the IR chain order parameter, S_θ, distinctly changes across the H_{II} + L_α coexistence range (vide supra). Because of this different sensitivity, some of the S_θ isotherms indicate a broader transition range (which refers to gel + H_{II} and H_{II} + L_α) than the respective COG($\nu_s(CH_2)$) graphs (referring virtually only to gel + H_{II}, compare, e.g., Figure 4a,b, $T = 20$ °C). Moreover, the samples in which gel and H_{II} phases coexist at low RH show a distinct chain melting event at low RH values at which gel domains completely melt into the fluid state (see, for example, the stepwise increase of COG($\nu_s(CH_2)$) in Figure 3c, $T = 20$ °C). These RH values were attributed to the liquidus line of the gel + H_{II} phase coexistence range or, equivalently, to the critical RH value of three phase coexistence gel + L_α + H_{II}.

Inspection and comparison of the phase diagrams reveals the following properties: (i) The nonionic detergents of the $C_{12}E_n$ type promote the formation of the inverse hexagonal phase, H_{II}, at reduced hydration and above a critical temperature, T_{crit}, i.e., in the left upper corner of the phase diagram. Neither pure POPC nor the pure detergents form a H_{II} phase at the conditions studied. Therefore, its formation represents a property of the mixtures rather than the dominant behavior of one component. The appearance of the H_{II} phase after mixing two L_α phase-forming lipids, namely, dioleoyl-PC (DOPC) and monoacylglycerol, was previously reported.[26] (ii) Increasing amounts of detergent in the mixtures extend the range of the H_{II} phase in the direction of higher RH values. $C_{12}E_2$ shows the strongest effect. (iii) $C_{12}E_2$ stabilizes the gel phase as compared with $C_{12}E_6$ and $C_{12}E_4$ at the same concentration as indicated by the higher onset temperature of chain melting at equal RH (see also Figure 7). (iv) Despite these differences, the phase diagrams show very similar properties for $C_{12}E_2$, $C_{12}E_4$, and $C_{12}E_6$ when mixed with POPC. Hence, the variation of the EO chainlength between n = 2 and 6 only weakly affects the phase properties of the lipid/detergent mixtures. (v) All studied systems form membranes at full hydration (RH = 100%) whereas the pure detergents assemble either into lamellae ($C_{12}E_4$, L_α phase[27,28]) or into micelles ($C_{12}E_6$, L_1 phase;[27] $C_{12}E_2$, L_2 phase[29]) at RH = 100%.

Structure of Pure $C_{12}E_4$ and $C_{12}E_6$ in the Solid State. Crystalline polyoxyethylene chains have a 7_2 helical conformation that contains seven EO (−O−CH_2−CH_2−) units within two turns. The internal rotations along the series of bonds O−CH_2−CH_2− are −trans−gauche−trans− (TGT). We will designate such a helical sequence of bonds by ...−O(T)−C(G)−C(T)−... (methylene hydrogens are omitted, T and G refer to the conformation, trans or gauche, of the subsequent bond). The helical structure belongs to the factor group D($4\pi/7$) with A_2 and E_1 species being IR active, having the direction of the transition moments parallel and perpendicular to the helical axis, respectively.[16] The polarized IR spectra of solid $C_{12}E_4$ and $C_{12}E_6$ show a series of absorption bands of either parallel ($S_{IR} \approx 1$, $A_\perp \approx 0$) or perpendicular ($S_{IR} \approx -0.5$) linear dichroism (see Figure 11 and Table 1). Their frequencies and linear dichroism virtually agree with those of crystalline polyoxyethylene.[31] We conclude that the EO chains of the detergents exist in the helical conformation. The strong dichroism and the respective order parameter are compatible with helical axes, which orient in a perpendicular direction relative to the surface of the ATR crystal.

To characterize the conformation, packing mode, and orientation of the alkyl chains of the detergents, we use two couples of vibrations, namely, the antisymmetric and symmetric CH_2

TABLE 1: Selected IR Active Modes of $C_{12}E_m$ ($m = 2, 4$) in Solid and Fluid Phases[a]

		$C_{12}E_4$[b]			$C_{12}E_2$		
		solid[e]		fluid[e]	solid[e]		fluid[e]
chain[c]	mode[d]	cm^{-1}	S_{IR}	cm^{-1}	cm^{-1}	S_{IR}	cm^{-1}
ethoxy	ν(OH)	3194	−0.5	3447	3235	−0.3	3423
		3327	>0.3		3333	0.3	
	$\nu_{as}(CH_2)_{EO}$			2930br			
	$\nu_s(CH_2)_{EO}$			2868			
	$\delta(CH_2)_{EO}$	1464		1457	1493[h]	<−0.4	1455
	$\gamma_W(CH_2)_{EO}$	1363[f]	−0.5	1350	1368	>0.5	1368
		1348[f]	1		1323	0.1	1351
	$\gamma_T(CH_2)_{EO}$	1280	−0.5	1299br			1323
		1242[f]	1	1284	1231[g]	>0.5	1249
		1230[f]	−0.5	1248	1228[g]	<−0.3	
	ν(CC)	1146	−0.5	1141sh	1145	0.1	1138
		1129	>0.5				
		1123	<0				
		1116		1118			1122
		1109		1107			1112
		1101					
	ν(CO)	1080			1078	1	
		1068		1070sh	1070	1	1069
		1062			1055,1047	−0.5	
	$\gamma_R(CH_2)_{EO}$	963[f]	>0.7		971[h]	<−0.3	
		939[f]	>0.7	947			933
	$\gamma_R(CH_2)_{EO}$	851	−0.5	886	862[g]	−0.4	891
	$+\nu$CO	845	<−0.4	840w			
alkyl	$\nu_{as}(CH_2)$	2916	0.15		2916	−0.25	2924
	$\nu_s(CH_2)$	2850	−0.5		2850	−0.45	2855
	$\delta(CH_2)$	1472	−0.5	1467	1471	−0.4	1467
	$\gamma_R(CH_2)$	716	0.35		717	−0.2	721

[a] For assignments see refs 25 and 37. [b] $C_{12}E_6$ shows very similar band positions and IR order parameters as $C_{12}E_4$. [c] EO chain or alkyl chain of $C_{12}E_m$. [d] Assignments: ν-stretches with subscript s (symmetrical) or as (antisymmetrical); γ deformation mode with subscript W (wagging), T (twisting), and R (rocking); δ-bending vibration. Note that especially the vibrations of the EO chains represent complex mixtures of different modes. Here, we refer only to the mode that gives the highest contribution. [e] Conditions: solid, RH = 50% and $T = 4$ °C; fluid, RH = 86% and $T = 25$ °C. [f] Characteristic for the helical conformation of the EO chain with O(T)−C(G)−C(T)−. [g] Characteristic for the terminal O(T)−C(G)−C−OH conformation. [h] Characteristic for the extended O(T)−C(T)−C(T)− conformation.

stretches, $\nu_{as}(CH_2)$ and $\nu_s(CH_2)$, respectively, and the CH_2 rocking and bending modes, $\gamma_r(CH_2)$ and $\delta(CH_2)$, respectively (see Table 1, Figure 11, and refs 13 and 32 for details). The frequencies of the latter two modes (~716 and 1472 cm^{-1}), their strong linear dichroism, and the absence of band splits (the overlap weak band at 1464 cm^{-1} was assigned to vibrations of the EO chain, see Table 1) are typical for the predominantly parallel arrangement of the zigzag planes of the all trans chains in an orthorhombic parallel packing motif.[33]

The IR order parameters of the $\nu_s(CH_2)$ and $\delta(CH_2)$ bands of $C_{12}E_4$ are negative (i.e., $2A_\perp > A_{||}$, see Figure 11 and Table 1) whereas those of $\nu_{as}(CH_2)$ and $\gamma_r(CH_2)$ are positive (i.e., $2A_\perp < A_{||}$). The transition moments of the former two modes, $\nu_s(CH_2)$ and $\delta(CH_2)$, virtually point along the bisector of the H−C−H bond angle whereas the transition moment of the latter two vibrations, $\nu_{as}(CH_2)$ and $\gamma_r(CH_2)$, orients along the interconnecting line between both hydrogens.[13] Consequently, the different linear dichroism of both types of vibrations indicates (i) the absence of rotational disorder about the chain axes and (ii) a tilt of the chain axes relative to the normal of the ATR crystal. The normalized longitudinal order parameters, $S_z = S_\theta / S_\theta^{max} \approx 0.5(3\cos^2\theta_{zn} - 1)$, provides an estimation of the tilt angle of the chain axes with respect to the layer normal, θ_{zn}.[13,14,32] With a maximum value of $S_\theta^{max} \approx 0.7-1$,[14] one obtains $\theta_{zn} \approx 35-40°$ for $C_{12}E_4$ and $C_{12}E_6$ (data not shown). Previous studies showed that the alkyl chain tilted away from the EO helix axis as a consequence of a helical/extended diblock conformation of $C_{12}E_m$ with $m > 3$.[34] Space-filling packing presumes $\cos\theta_{zn} \approx A_{alkyl}/A_{EO}$, where A_{alkyl} and A_{EO} denote the effective cross-sections of the extended alkyl and helical EO chains, respectively. With $A_{alkyl} \approx 0.19$ nm^2 and $\theta_{zn} \approx 35-40°$, one obtains $A_{EO} \approx 0.23-0.25$ nm^2, a value that appears reasonable as the cross-section of a 7_2 helix.[16]

Structure of Pure $C_{12}E_2$ in the Solid State. The differences between the IR spectra of solid $C_{12}E_2$ and of solid $C_{12}E_4$ (compare Figures 11 and 12) refer mainly to the absorption bands of the EO units (Table 1). For example, $C_{12}E_2$ shows bands at 971 and 862 cm^{-1}, which are associated with ...−C(T)−C(T)−O(T)−C(T)−C(T)−O−... and ...−O(T)−C(G)−C−OH fragments, respectively.[30] In contrast, $C_{12}E_4$ (and $C_{12}E_6$) shows a band around 939 cm^{-1}, which is absent in the spectrum of $C_{12}E_2$. This feature is due to a rocking mode of helical ...−O−C(G)−C(T)−O(T)−C(G)−... fragments. The detergent $C_{12}E_2$ does not show, unlike $C_{12}E_4$, a band at 1242 cm^{-1} because of antisymmetric CH_2 twisting modes of interior ...−O(T)−C(G)−C(T)−... units but possesses only bands at 1230 and 1228 cm^{-1} due to terminal −O(T)−C(G)−C−OH groups.[30] A weak band at 1493 cm^{-1} was tentatively attributed to CH_2 bending vibrations of EO units in the trans conformation.[30] We confirm this assignment because the band disappears in the IR spectrum of $C_{12}E_2$-d_8 owing to the isotopic shift of the EO methylenes (not shown). The respective IR order parameter, $S_{IR} \approx -0.45$, is compatible with stretched EO chains, which virtually align along the normal of the ATR surface. The respective transition moment is assumed to make the right angle with the long axis of an EO chain in the all trans conformation. Hence, spectral analysis and linear dichroism reveal the stretched all trans conformation of the EO units in crystalline $C_{12}E_2$ in contrast to the helical conformation of the EO chains in crystalline $C_{12}E_4$ and $C_{12}E_6$.

The wavenumbers and IR order parameters of the vibrational modes of the alkyl methylenes of $C_{12}E_2$ (apply the same arguments as for $C_{12}E_4$) give rise to the conclusion that the stretched alkyl chains arrange into an orthorhombic parallel subcell. The chain axes orient nearly parallel with respect to the normal of the ATR surface ($0° < \theta_{zn} < 20°$); thus, the vibrational characteristics of crystalline $C_{12}E_2$ are compatible with a layered structure in which the alkyl and EO chains adopt the trans conformation with the exception of the terminal hydroxyl part.

In summary, the conformational properties of the EO chain of $C_{12}E_m$ detergents may be elucidated by the conformational competition between the EO chain, which intrinsically favors the helical structure, and the alkyl chain, which favors the extended all trans structure. Our results agree with previous findings that the molecular conformation of the EO chains of C_mE_n detergents in the solid state changes from the helix dominative β form to an extended γ form, as the number of EO units, m, is decreased below four.[35] This critical value corresponds approximately to one turn of the 7_2 helix.

Solid−Solid Coexistence in Mixed Lipid/Detergent Membranes. The IR spectra of mixtures of POPC/$C_{12}E_4$ at $T = 4$ °C and $R_{D/L} = 1$ (Figure 11) and of POPC/$C_{12}E_6$ at $R_{D/L} = 1$ and 0.5 (not shown) indicate solid−solid coexistence of crystalline detergent with a lipid-rich gel phase. The weak but clearly

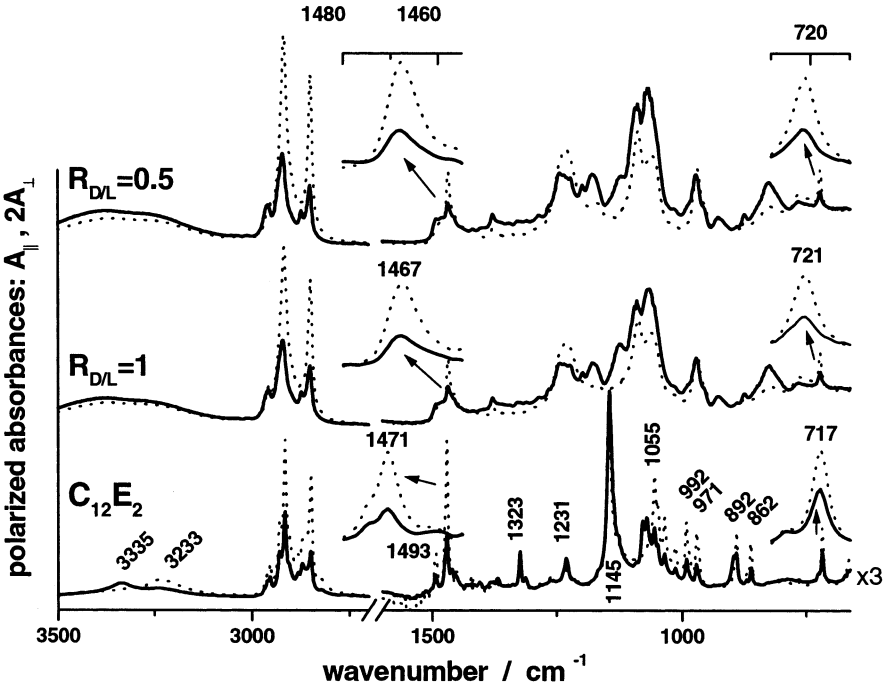

Figure 12. Polarized IR spectra, $A_{||}(\nu)$ and $2A_{\perp}(\nu)$, of the detergent $C_{12}E_2$ and of POPC/$C_{12}E_2$ mixtures with $R_{D/L} = 0.5$ and 1 ($T = 10$ °C, RH = 50%). The insertions amplify the spectral regions of the $\delta(CH_2)$ and $\gamma_R(CH_2)$ modes (see text).

visible parallel polarized band at 1198 cm^{-1} was unequivocally assigned to the $k = 1$ component of the wagging progression of the palmitoyl chains of the lipid, which exist in the extended all trans conformation. Several strongly polarized bands of the EO chains protrude against the background of the lipid spectrum and show the same essential properties (band positions and linear dichroism) as the pure detergents in the crystalline state. The methylene bending and rocking bands of the mixture represent doublets (see insertions in Figure 11), which can be explained by the superposition of respective modes of both components ($\delta(CH_2)$: POPC at 1467 cm^{-1} and $C_{12}E_4$ at 1472 cm^{-1}; $\gamma_R(CH_2)$: POPC at 721 cm^{-1} and $C_{12}E_4$ at 716 cm^{-1}). An alternative interpretation in terms of split $\delta(CH_2)$ and $\gamma_R(CH_2)$ bands owing to crystal field splitting in an orthorhombic perpendicular packing motif of the chains appears not reasonable in view of the essentially unperturbed spectral properties of the components in the mixture.

Mixed Lipid/Detergent Membranes in the Gel and in the Fluid State. The sharp bands that are characteristic for the crystalline detergent disappear in the mixtures POPC/$C_{12}E_2$ at $R_{D/L} = 1$ and 0.5 (Figure 12) and POPC/$C_{12}E_4$ at $R_{D/L} \leq 0.5$ (Figure 11). Instead, the respective IR spectra combine features of the detergents with EO chains in a different state with that of POPC with frozen acyl chains. The positions of the CH_2 bending and rocking bands of the hydrocarbon chains at 1467 and 721 cm^{-1}, respectively, are typical for a hexagonal packing motif of the hydrocarbon chains. Both components obviously form mixed membranes in the gel phase.

We calculated polarized difference spectra of the two component systems and of pure POPC to filter out the spectrum of the detergent in the mixture together with subtle alterations of the lipid spectrum owing to lipid/detergent interactions (Figure 13a−e). The difference spectrum POPC/$C_{12}E_2$−POPC (Figure 13a) reveals a higher degree of molecular ordering of the lipid in the presence of the detergent as compared to the pure lipid. The CH_2 wagging progression bands and the CO−O−C antisymmetric stretching mode (near 1173 cm^{-1}) of the palmitoyl chains of POPC are more intense in the presence of $C_{12}E_2$. Obviously, a higher fraction of palmitoyl chains exists in the all trans conformation when the detergent was added to the lipid. The residual absorbance in the spectral range of the antisymmetric CO−P−OC stretching band near 824 cm^{-1} reflects the fact that also the phosphate groups are more ordered in the mixture than in the pure POPC membrane. Hence, the spectra indicate that $C_{12}E_2$ exerts a condensing/ordering effect on the lipid. This result is compatible with the upwards shift of the chain melting transition of the POPC/$C_{12}E_2$−POPC mixture discussed above.

Moreover, the difference spectrum shows strong, parallel polarized bands at 1127 and 1064 cm^{-1} for $C_{12}E_2$ in the gel state membranes (Figure 13a). These features are due to coupled modes of the EO skeleton with a predominant fraction of C−C and C−O stretches and with only a weak contribution of CH_2 rocking vibrations.[16] This result reports about relatively ordered EO chains, which orient predominantly along the membrane normal. The difference spectra of detergents with longer EO chains show similar features in this spectral range (Figure 13b) not only in the solid state but in the fluid phases as well (Figure 13c−e). The intensity of an additional band near 1086 cm^{-1} raises with increasing number of EO groups. It originates probably from vibrations of interior EO units. Normal coordinate analyses of $H(OCH_2CH_2)_2OH$ and $CH_3OCH_2CH_2OH$ fragments in the O(T)−C(G)−C−OH conformation predict the symmetrical stretches ν_s(OCC) and ν_s(COC) around 1125 and 1060 cm^{-1}, respectively, whereas for longer EO fragments additional modes appear near 1090 cm^{-1} [16] in agreement with our assignment.

Note that the overlap absorption bands of −O−C−C− skeleton modes of the detergents in the lipid/detergent mixtures are distinctly more structured than in the spectrum of the pure detergents (compare Figures 1 and 13). Reduced bandwidths of component bands reflect relatively narrow distributions of conformational states; thus, the IR difference spectra suggest an increased molecular ordering of the EO chains, which reside in the polar region of the membranes. This conclusion is confirmed by the linear dichroism of these bands. For example,

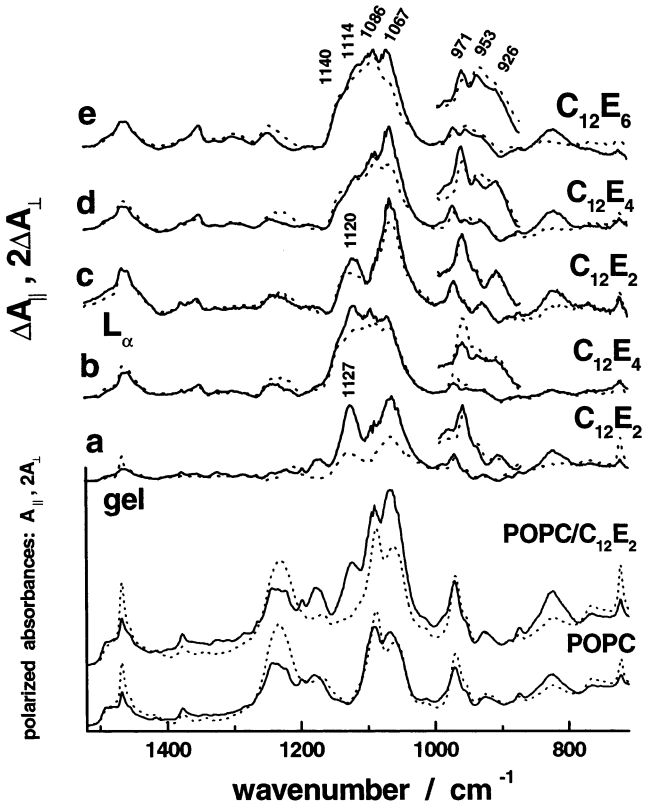

Figure 13. Selected region of the polarized IR spectrum, $A_{||}(\nu)$ (solid line) and $2A_\perp(\nu)$ (dotted line), of POPC and of a POPC/$C_{12}E_2$ mixture (below, $R_{D/L} = 1$, $T = 10$ °C, RH = 50%). Traces a−e are difference spectra, $\Delta A_i = A_i$(mixture) − kA_i(POPC) ($i = ||, \perp$) where the normalization factor k was chosen to compensate the intensity of the C═O stretching mode. The difference spectra refer to mixtures of the lipid with detergents in the gel phase, $C_{12}E_2$ (a, $R_{D/L} = 1$, $T = 10$ °C, RH = 50%) and $C_{12}E_4$ (b, $R_{D/L} = 0.5$, $T = 10$ °C, RH = 30%), and in the L_α phase, $C_{12}E_2$ (c, $R_{D/L} = 1$, $T = 30$ °C, RH = 80%), $C_{12}E_4$ (d, $R_{D/L} = 1$, $T = 30$ °C, RH = 80%), and $C_{12}E_6$ (e, $R_{D/L} = 1$, $T = 30$ °C, RH = 80%). The insertions amplify the polarized difference spectra in two spectral regions. Wavenumbers of peak positions are given in units of cm^{-1}.

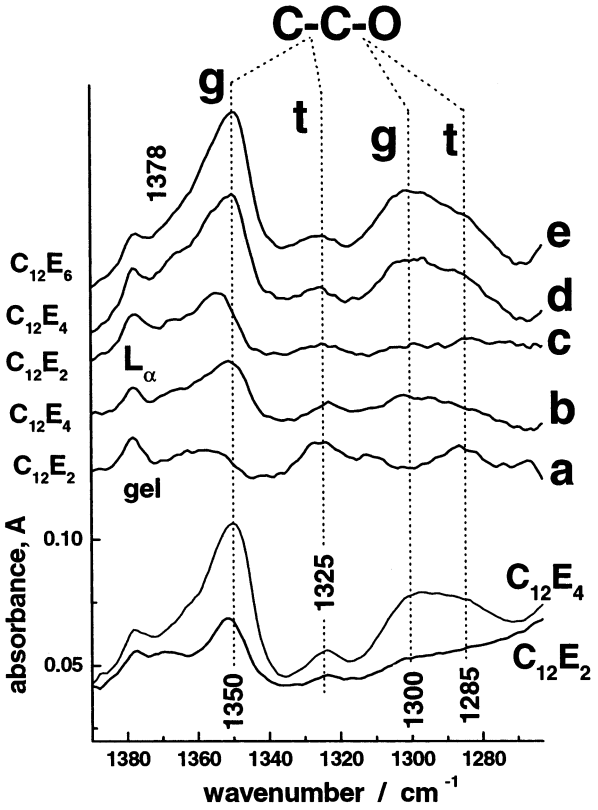

Figure 14. Region of the conformational key bands in the sum spectrum, $A(\nu) = A_{||}(\nu) + 2.55A_\perp(\nu)$, of pure $C_{12}E_2$ and $C_{12}E_4$ (spectra below; $T = 25$ °C, RH = 50%) and of the detergents incorporated in POPC membranes (spectra a−e). Traces a−e are calculated using the difference spectra a−e shown in Figure 13. See Figure 13 caption for details. Band positions are given in units of cm^{-1}. The peak at 1378 cm^{-1} refers to the "umbrella" vibration of the terminal CH_3 group. Its intensity can serve as an internal standard for comparison between the different spectra.

the relatively strong parallel linear dichroism of the bands at 1127 and 1064 cm^{-1} of $C_{12}E_2$ with IR order parameters of $S_{IR} \approx 0.3-0.5$ indicates a high degree of ordering of the EO chains in the gel state of the mixed membranes (Figure 13a).

In aqueous solution, polyoxyethylene chains with more than two EO units have conformational preference of the gauche conformation around the OC−CO bond (C−C) and preference of the trans conformation around the CC−OC bond (C−O) (see ref 36 and references therein). Well-defined key bands of the C−C bond at 1355−1350 cm^{-1} for the gauche and at 1335−1325 cm^{-1} for the trans conformation and key bands of the C−O bond at 1300−1297 cm^{-1} (gauche) and at 1288−1285 cm^{-1} (trans) allow the conformational analysis of partly disordered EO chains in solution by means of IR spectroscopy.[36] The key absorption bands are associated with the CH_2 wagging (C−C) and the CH_2 twisting (C−O) mode (see Table 1).

Figure 14 shows the spectra of pure detergents in the fluid phase and of detergents in POPC membranes in the region of the conformational key bands. The strong intensity of the $\gamma_W(CH_2)_{EO}$(gauche) band near 1350 cm^{-1} reflects the preference of the C−C bond for the gauche conformation. The difference spectra a−e refer to the detergent in POPC membranes (see above and also Figure 13 for details). The spectra of the pure detergents and of detergents inserted into the fluid membrane are very similar in the region of the $\gamma_W(CH_2)_{EO}$ bands indicating similar populations of gauche and trans conformers of the C−C bonds. We conclude that the EO chains exist in a similar conformational state. The intensity of the $\gamma_W(CH_2)_{EO}$(trans) band near 1325 cm^{-1} is nearly independent of the length of the EO chain (compare spectra c−e) whereas that of the gauche band, $\gamma_W(CH_2)_{EO}$(gauche), increases with the EO chain length, $n = 2, 4, 6$. This result implies an increasing fraction of gauche conformers of the C−C bond with increasing EO chain length and thus a higher degree of disorder. On the other hand, the fraction of gauche conformers clearly decreases in the gel phase, especially for $C_{12}E_2$. The C−C and also the C−O linkages exist predominantly in the trans conformation here. The latter conclusion results from the relatively strong intensity of the $\gamma_T(CH_2)_{EO}$(trans) band near 1285 cm^{-1} (compare spectra a and c of Figure 14c). Hence, most of the EO chains of $C_{12}E_2$ adopt the stretched all trans conformation in the mixed gel phase.

Summary and Conclusions

The main aim of this study was to establish the lyotropic properties of POPC/$C_{12}E_n$ mixed systems in terms of RH-T phase diagrams and to characterize the molecular architecture of the amphiphilic aggregates using IR linear dichroism spectroscopy. Mixtures of the phospholipid POPC and nonionic surfactants of the $C_{12}E_n$ type ($n = 2, 4, 6$) assemble into fluid bilayer membranes at excess water conditions. After they dehydrate, the lamellae transform into the inverse hexagonal phase (H_{II}) at temperatures above a critical value $T > T_{crit}$, the extension of which in the phase diagrams increases with raising

detergent concentrations. The formation of the H_{II} phase represents an exclusive property of the mixture because neither pure POPC nor the pure detergents form the H_{II} phase at these conditions. It reflects specific cross-interaction between the components, which imbalance the lateral forces acting within the polar and apolar region of the membranes and finally cause the bending of the layers into thermodynamically stable water-inside hexagons.

At temperatures below a critical value, $T < T_{crit}$, dehydration of the mixed membranes induces the transition from the fluid liquid crystalline phase into the solid phase, which is characterized by stretched all-trans methylene chains of the components. $C_{12}E_6$ tends to demix into crystalline domains. The respective EO chains adopt the helical conformation with helical axes pointing along the membrane normal. This conformation is also characteristic for the pure detergents with four and six EO units. In contrast, the short EO chains of $C_{12}E_2$ prefer the all-trans conformation in crystals of the pure detergent. In mixed POPC/$C_{12}E_2$ membranes, however, the EO chains exist in a partially disordered conformation where mixed gel state domains are formed. $C_{12}E_4$ shows similar properties at low concentrations. At higher concentrations, it demixes into crystalline domains, which resemble those of $C_{12}E_6$.

$C_{12}E_2$ shows special properties not only with regard to the conformation of the EO chains in solid systems. In mixed membranes, it increases T_{crit} and it extends the range of the H_{II} phase to higher RH as compared with the effect of the detergents with longer EO chains. In other words, $C_{12}E_2$ stabilizes the gel phase and it is the most effective among the studied detergents with respect to their ability to promote the formation of the H_{II} phase upon dehydration.

Linear dichroism spectroscopy is well-suited to differentiate between fluid and solid phases using band positions of characteristic marker bands on one hand and between lamellar and nonlamellar phases using the dichroic properties of the IR spectrum on the other hand. In a methodical respect, this study extends previous investigations on the lyotropic phase behavior of pure lipids[17,15] to lipid/detergent mixtures.

Acknowledgment. This work has been supported by Bundesministerium für Bildung und Technologie (BMBF Grant DUBLEI 03).

References and Notes

(1) Guo, J. D.; Zerda, T. W. *J. Phys. Chem. B* **1997**, *101*, 5490.
(2) Siminovitch, D. J.; Wong, P. T. T.; Mantsch, H. H. *Biochemistry* **1987**, *26*, 3277.
(3) Wong, P. T. T.; Siminovitch, D. J.; Mantsch, H. H. *Biochim. Biophys. Acta* **1988**, *947*, 139.
(4) Winter, R.; Czeslik, C. *Z. Kristallogr.* **2000**, *215*, 454.
(5) Parsegian, V. A.; Fuller, N.; Rand, R. P. *Proc. Natl. Acad. Sci. U.S.A.* **1979**, *76*, 2750.
(6) Koenig, B. W.; Strey, H. H.; Gawrisch, K. *Biophys. J.* **1997**, *73*, 1954.
(7) Binder, H.; Dietrich, U.; Schalke, M.; Pfeiffer, H. *Langmuir* **1999**, *15*, 4857.
(8) Binder, H.; Anikin, A.; Kohlstrunk, B.; Klose, G. *J. Phys. Chem. B* **1997**, *101*, 6618.
(9) Binder, H.; Anikin, A.; Lantzsch, G.; Klose, G. *J. Phys. Chem. B* **1999**, *103*, 461.
(10) Wrigley, A. N.; Stirton, A. J.; Horward, E. J. *Org. Chem.* **1960**, *25*, 4391.
(11) Schnabel, R. *J. Labelled Compd. Radiopharm.* **1992**, *21*, 91.
(12) Harrick, N. J. *Internal Reflection Spectroscopy*; Wiley: New York, 1967.
(13) Binder, H.; Schmiedel, H. *Vib. Spectrosc.* **1999**, *21*, 51.
(14) Binder, H.; Gawrisch, K. *J. Phys. Chem. B* **2001**, *105*, 12378.
(15) Binder, H. *Appl. Spectrosc. Rev.*, accepted for publication.
(16) Miyazawa, T.; Fukushima, K.; Ideguchi, Y. *J. Phys. Chem.* **1962**, *37*, 2764.
(17) Binder, H.; Gawrisch, K. *Biophys. J.* **2001**, *81*, 969.
(18) Klose, G.; Eisenblätter, S.; König, B. *J. Colloid Interface Sci.* **1995**, *172*, 438.
(19) Seddon, J. M.; Cevs, G.; Marsh, D. *Biochemistry* **1983**, *22*, 1280.
(20) Funari, S. S. *Eur. Biophys. J.* **1998**, *27*, 590.
(21) Gutberlet, T.; Dietrich, U.; Klose, G.; Rapp, G. *J. Colloid Interface Sci.* **1998**, *203*, 317.
(22) Seelig, A.; Seelig, J. *Biochemistry* **1974**, *13*, 4839.
(23) Klose, G.; Levine, Y. L. *Langmuir* **1999**, *16*, 671.
(24) Funari, S. S.; Klose, G. *Chem. Phys. Lipids* **1995**, *75*, 145.
(25) Binder, H.; Kohlstrunk, B.; Heerklotz, H. H. *J. Colloid Interface Sci.* **1999**, *220*, 235.
(26) Nilsson, A.; Holmgren, A.; Lindblom, G. *Biochemistry* **1991**, *30*, 2126.
(27) Mitchell, D. J.; Tiddy, G. J. T.; Waring, L.; Bostock, T.; McDonald, M. P. *J. Chem. Soc., Faraday Trans. 1* **1983**, *79*, 975.
(28) Mädler, B.; Binder, H.; Klose, G. *J. Colloid Interface Sci.* **1998**, *202*, 124.
(29) Conroy, J. P.; Hall, C.; Lang, C. A.; Rendall, K.; Tiddy, G. J. T.; Walsh, J.; Lindblom, G. *Colloid Polym. Sci.* **1990**, *82*, 253.
(30) Matsuura, H.; Fukuhara, K.; Tamaoki, H. *J. Sci. Hiroshima University, Ser. A* **1985**, *49*, 89.
(31) Kimura, N.; Umemura, J.; Hayashi, S. *J. Colloid Interface Sci.* **1996**, *182*, 356.
(32) Binder, H. *Vib. Spectrosc.* **1999**, *21*, 151.
(33) Snyder, R. G. *J. Mol. Spectrosc.* **1961**, *7*, 116.
(34) Dorset, D. L. *J. Colloid Interface Sci.* **1983**, *96*, 172.
(35) Matsuura, H.; Fukuhara, K. *J. Phys. Chem.* **1987**, *91*, 6139.
(36) Wahab, S. A.; Matsuura, H. *Phys. Chem. Chem. Phys.* **2001**, *3*, 4689.